Sound Attenuation by Hearing Aid Earmold Tubing

Mads J. Herring Jensen
Widex A/S
Ny Vestergaardsvej 19, DK-3500 Vaerloese, Denmark, mjj@widex.dk

Abstract: In this study we model the sound attenuation properties of a hearing aid earmold tube. The model includes thermoviscous acoustic effects and it couples structural vibrations to the external acoustic field. Moreover, the finite element domain is coupled at two boundaries with an electroacoustic model of a hearing aid and an acoustic 2-cc coupler.

Keywords: Thermoviscous, acoustic, impedance, boundary condition

1 Introduction

A major problem in high power hearing aids is feedback and mechanical stability. One of the possible sources of feedback may be the sound radiating from the plastic tubing that connects the hook on the hearing aid (behind/on the ear) to the earmold (located in the ear). Sound radiating through the tubing may be picked up by the hearing aid microphone and create feedback. The current modeling work is inspired by the experimental work of Flack *et al.* [6]. Using Comsol Multiphysics we model the same experimental setup which they used to measure the sound attenuation of the tubing. In the following, we, firstly, present experimental set-up and the finite element (FEM) model set up. Secondly, we present the governing equations for sound propagation in a fluid including thermoviscous losses and for sound vibrations in an elastic solid. We also present the boundary conditions (BCs) used to couple the FEM domain to an electroacoustic equivalent of a hearing aid and a coupler. Then the modeling results are presented, and, finally, we give some conclusions.

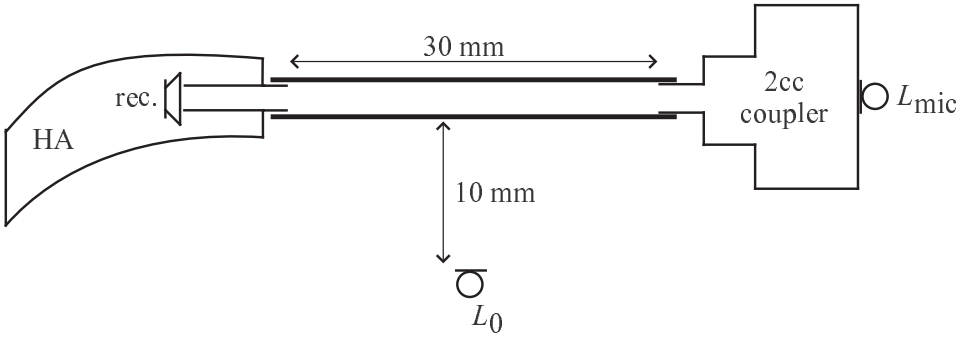

Figure 1: Schematic of the experimental set-up used by Flack *et al.* [6] to measure sound attenuation. The system includes hearing aid (HA), 2-cc coupler, receiver (rec.), coupler microphone L_{mic}, external microphone L_0 , and the 30 mm earmold tube.

2 Experimental set-up

In the experiments performed by Flack *et al.*, a rubber tube of length 30 mm is connected in one end to a HA and in the other end to a 2-cc coupler. The experiment is performed in a soundproof test box. The signal played by the hearing aid receiver is recorded at the coupler microphone L_{mic} and on the outside at the microphone L_0. The experimental set-up is depicted in Fig. 1.

3 Model set-up

In order to model the the sound attenuation of the earmold tubing we have chosen to mimic the experimental set-up described above. The computational domain is depicted in Fig. 2 including selected dimensions. The tube has length L, inner diameter R, and outer diameter $R + dR$. To reduce the computational cost the system has been simplified. Firstly, we have used an axisymmetric model and, secondly, the hearing aid and coupler are modeled by electroacoustic equivalents on the inlet and outlet boundaries. The coupling is performed using acoustic impedance BCs (described below). The outer acoustic domain is truncated using a perfectly matched layer region mimicking an open boundary (also described below). The system of equations and BCs is implemented using the Comsol scripting language into Matlab.

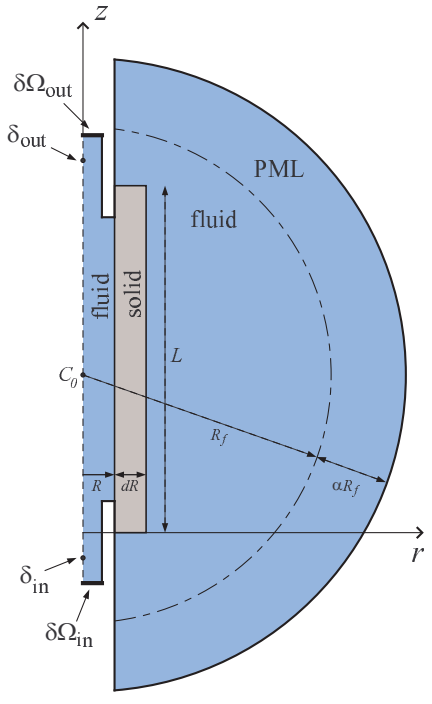

Figure 2: Schematic representation of the FEM part of the system comprising fluid, solid, and perfectly matched layer (PML) domain. The rubber tube has inner radius R, outer radius $R + dR$, length L, inlet boundary $\partial\Omega_{in}$, and outlet boundary $\partial\Omega_{out}$. The two points δ_{in} and δ_{out} are used to implement point constraints.

4 Governing equations

In the fluid areas we solve the full thermoviscous acoustic problem assuming time harmonic variation of the dependent variables. The problem is defined by the linearized Navier-Stokes equation

$$i\omega\rho_0 u_i = -\nabla_i p + (\lambda+\mu)\nabla_i(\nabla_j u_j) + \mu\nabla_j\nabla_j u_i, \tag{1}$$

the continuity and constitutive equation

$$i\omega\left(\frac{p}{p_0} - \frac{T}{T_0}\right) = -\nabla_i u_i, \tag{2}$$

and the energy equation

$$i\omega\rho_0 C_p T = \kappa\nabla_i\nabla_i T + i\omega p, \tag{3}$$

where p is the acoustic pressure, T the excess temperature, u_i the acoustic velocity variation component, ω the angular frequency, p_0 the static pressure, T_0 the static temperature, μ the dynamic viscosity, λ the dilatational viscosity, C_p the specific heat at constant pressure, and κ the heat conduction coefficient. Further details are found in Refs. [2, 1, 9, 5, 8].

In the solid domain we solve for the displacement field U_i in a linear elastic solid

$$-\omega^2\rho_0 U_i = \nabla_j\sigma_{ij} \tag{4}$$

where we again assume time harmonic variations, and σ_{ij} is the stress tensor. To mimic the lossy properties of the elastic solid we introduce a complex Young's modulus $\tilde{E} = E(1 + i\eta)$, where η is the loss factor. In this study we assume that it is not necessary to model viscoelastic properties of the tubing and that η is not frequency dependent.

5 Perfectly matched layers

In the perfectly matched layers (PMLs) region we introduce a change of independent variables $x_i \rightarrow Z_{x_i}$. The variables are changed to complex valued and chosen such that they are continuous on the boundary. The new complex variables introduce a damping of the outgoing and incoming waves. With reference to Fig. 2 a set of coordinates that introduce absorption in the

spherical direction are defined by

$$\ell = \frac{|\boldsymbol{C}_0 - \boldsymbol{x}| - R_f}{\alpha R_f} \tag{5}$$

$$\tilde{R} = R_f + \ell^n \frac{c}{f}(1-i) \tag{6}$$

$$Z_{x_j} = \frac{\tilde{R}(x_j - x_0)}{|\boldsymbol{C}_0 - \boldsymbol{x}|}, \quad j = 1, 2 \tag{7}$$

where $\boldsymbol{C}_0 = (0, z_0)$, $[x_i] = (r, z)$, n is an exponent that controls the amount of damping, ℓ is the local radial coordinate in the PML, c the speed of sound, and f the frequency. For further details see Refs. [3, 11, 4, 7].

This change of variables is straight forward when the governing equations are formulated in the weak form. The main task when implementing the new coordinates in the PML region is to calculate the Jacobian J and its inverse J^{-1}. When this is done the integrals in the weak formulation may be changed as follows

$$\int_\Omega f(x_i, \frac{\partial}{\partial x_i})dV \rightarrow \int_{\tilde{\Omega}} f(Z_{x_i}, \frac{\partial}{\partial Z_{x_i}})d\tilde{V} = \int_\Omega f(Z_{x_i}(x_i), J^{-1}_{ji}\frac{\partial}{\partial x_j})|J|dV. \tag{8}$$

6 Boundary conditions

Fluid-solid: On the fluid-solid boundary we impose continuity of the displacement field $i\omega U_i = u_i$ and of the normal stress. This is achieved by introducing a Lagrange multiplier $\boldsymbol{\lambda} = (\lambda_u, \lambda_v)$ and defining

$$\boldsymbol{n}_2 : \boldsymbol{\sigma} = \boldsymbol{\lambda} \tag{9}$$

$$\boldsymbol{n}_1 : \boldsymbol{S} = -\boldsymbol{\lambda} \tag{10}$$

$$\tilde{\boldsymbol{\lambda}} \cdot (\boldsymbol{u} - i\omega \boldsymbol{U}) = 0. \tag{11}$$

where $\tilde{\boldsymbol{\lambda}}$ is the test function of the Lagrange multiplier, $\boldsymbol{\sigma}$ is the stress in the solid and $\boldsymbol{S}$ is the stress in the fluid. This yields a weak term on the solid-fluid boundary having the form

$$\int_{\partial\Omega} (\tilde{\boldsymbol{U}} - \tilde{\boldsymbol{u}}) \cdot \lambda dL + \int_{\partial\Omega} \tilde{\boldsymbol{\lambda}} \cdot (\boldsymbol{u} - i\omega \boldsymbol{U}) dL \tag{12}$$

Inlet and outlet: On the inlet and outlet boundaries we wish to couple the FEM model to an electroacoustic model (or two-port model). This idea is inspired by Stinson and Daigle [10]. On the inlet we have a two-port prescribing the relation between the electrical input on the receiver (current I_{rec} and voltage V_{rec}) and the acoustic output of the HA (pressure p_{in} and volume flow Q_{in}) given by

$$\begin{bmatrix} V_{rec} \\ I_{rec} \end{bmatrix} = \begin{bmatrix} A_{in} & B_{in} \\ C_{in} & D_{in} \end{bmatrix} \begin{bmatrix} p_{in} \\ Q_{in} \end{bmatrix} \tag{13}$$

where the matrix elements are frequency dependent. On the outlet we also use an electroacoustic equivalent of the 2-cc coupler and coupler microphone, which may be formulated as an acoustic impedance

$$Z_{out} = \frac{p_{out}}{Q_{out}}. \tag{14}$$

The two above acoustic conditions are imposed as weak constraints on the points δ_{in} and δ_{out} depicted on Fig. 2. On the inlet as

$$\begin{aligned} &\boldsymbol{u} - \lambda_1 \boldsymbol{u}_e = 0 \quad \text{on} \quad \partial\Omega_{in} \\ &\int_{\delta_{in}} (V - A_{in}P_{in}/\alpha_{in} - B_{in}Q_{in})\tilde{\lambda}_1 \, dP = 0 \\ &[\alpha_{in}, P_{in}, Q_{in}] = \int_{\partial\Omega_{in}} [1, p, \boldsymbol{u} \cdot \boldsymbol{n}] \, dA \end{aligned} \tag{15}$$

and on the outlet

$$\begin{aligned} &\boldsymbol{u} - \lambda_2 \boldsymbol{u}_f = 0 \quad \text{on} \quad \partial\Omega_{out} \\ &\int_{\delta_{out}} (P_{out}/\alpha_{out} - Z_{out}Q_{out})\tilde{\lambda}_2 \, dP = 0 \\ &[\alpha_{out}, P_{out}, Q_{out}] = \int_{\partial\Omega_{out}} [1, p, \boldsymbol{u} \cdot \boldsymbol{n}] \, dA \end{aligned} \tag{16}$$

where λ_1 and λ_2 are Lagrange multipliers and $\boldsymbol{u}_e$ and $\boldsymbol{u}_f$ are the non-evanescent eigensolutions to the thermoviscous acoustic problem on the inlet and outlet boundaries, respectively. It is here important to note that we need to use the eigensolutions formulation because the boundaries are not regarded as walls but rather as open semi reflecting boundaries.

7 Results

The model is firstly run for material parameters representative of the earmold tubing used on standard Widex hearing aids. With Young's modulus $E = 4.1 \cdot 10^7$ Pa, Poission's ratio $\sigma_p = 0.45$, density $\rho_s = 1220$ kg/m^3, and the loss factor estimated to $\eta = 0.019$.

The simulated results of a sound attenuation experiment are presented in Fig. 3 together with the experimental results of Flack *et al.*. Note that the materials used in the experiment do not match the simulated tube. The experimental results are presented as a rough order of magnitude estimate.

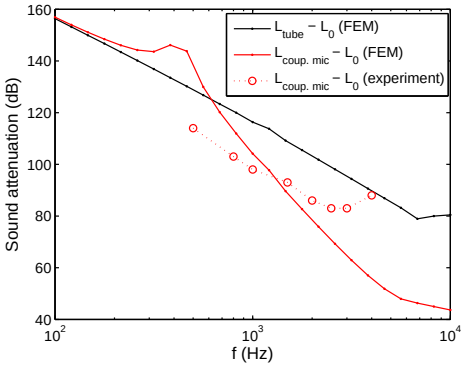

Figure 3: Simulated sound attenuation as function of frequency. The black line represents the direct sound attenuation measured from the center of the tube and the red line the attenuation measured with the coupler microphone. Experimental results of Flack *et al.* are presented with red bullets.

In Fig. 3 we note that the actual/correct sound attenuation calculated from within the tube center to outside the tube is larger than the one measured using the coupler microphone. This could indicate that the attenuations measured in the experiments are actually off by 30 dB for some frequencies.

In Fig. 4 we present the simulated attenuation for various values of the loss factor η, together with a simulated steel pipe, and again the experimental results (again only depicted as an order of magnitude estimate). From the figure we note that larger attenuation is naturally achieved for a more lossy material (increasing η) and for a more stiff material (steel). To numerically verify the experimental results of Flack *et al.* we might have to make some improvements to the model. Firstly, the loss factor might be frequency dependent and, secondly, the rubber might exhibit nonlinear viscoelastic properties not modeled here.

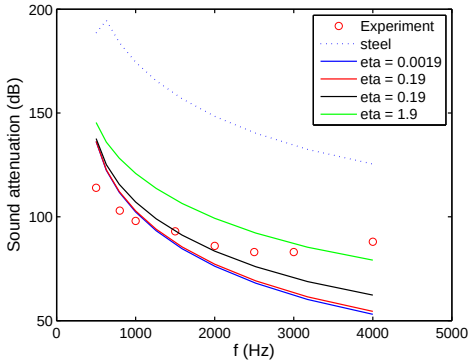

Figure 4: Simulated sound attenuation measured as $L_{couplermic.} - L_0$ for various values of the loss factor η and for a simulated steel tube.

As a final results we present the sound pressure level $L_p = 20\log(|p|/20 \cdot 10^{-6})$ field around the radiating earmold tube. The sound pressure level is depicted in Fig. 5 for the frequency $f = 1000$ Hz.

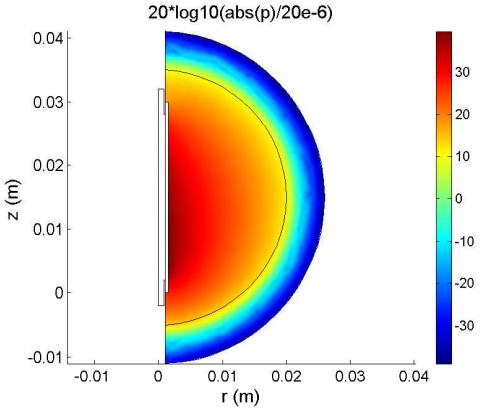

Figure 5: Sound pressure level L_p around the radiating tube for frequency $f = 1000$ Hz. Note the 50 dB attenuation over the PML layer.

8 Conclusion

The sound attenuation properties of earmold tubing have been investigated using an axisymmetric model of a thermoviscous acoustic fluid coupled with a linear elastic solid. The model comprises acoustic impedance boundary conditions that couple a FEM domain to an electroacoustic representation of a larger external acoustic system. This enables us to model a large acoustic system and only solve the details FEM model when relevant.

References

[1] W. M. Beltman, *Viscothermal wave propagation including acousto-elastic interaction, part I: Theory*, J. Sound Vib. **227** (1999), 555–586.

[2] W. M. Beltman, P. J. M. van der Hoogt, R. M. E. J. Spiering, and H. Tijdeman, *Implemantation and experimental validation of a new viscothermal acoustic finite element for acousto-elastic problems*, J. Sound Vib. **216** (1998), 159–185.

[3] J.-P. Berenger, *A perfectly matched layer for the absorbtion of electro magnetic waves*, J. Comp. Phys. **114** (1994), 185.

[4] A. Bermdez, L. Hervella-Nieto, A. Prieto, and R. Rodrguez, *An optimal perfectly matched layer with unbounded absorbing function for time-harmonic acoustic scattering problems*, J. Comp. Phys. **223** (2007), 469.

[5] D. T. Blackstock, *Fundamentals of physical acoustics*, (2000).

[6] L. Flack, R. White, J. Tweed, D. W. Gregory, and Y. M. Qureshi, *An investigation into sound attenuation by earmold tubing*, Brit. J. of Aud. **29** (1995), 237.

[7] T. K. Katsibas and C. S. Antonopopulos, *A general form of perfectly matched layers for three-dimensional problems of acoustic scattering in lossless and lossy fluid media*, IEEE **51** (2004), 964.

[8] L. D. Landau and E. M. Lifshitz, *Fluid mechanics, course of the theoretical physics*, **6** (2003).

[9] M. Malinen, M. Lyly, P. Rback, A. Krkkinen, and L. Krkkinen, *A finite element method for the modelling of thermo-viscous effects in acoustics*, ECCOMAS (2004).

[10] M. R. Stinson and G. A. Daigle, *Transverse pressure distributions in a simple model ear canal occluded by a hearing aid test fixture*, J. Acoust. Soc. Am. **121** (2007), 3689.

[11] F. L. Teixeira and W. C. Chew, *Perfectly matched layer in cylindrical coordinates*, IEEE proceeding.